Cu(II)-catalyzed oxidation of beta-amyloid peptide targets His13 and His14 over His6: Detection of 2-Oxo-histidine by HPLC-MS/MS.

ARTICLE *in* CHEMICAL RESEARCH IN TOXICOLOGY · JUNE 2002

Impact Factor: 3.53 · Source: PubMed

2 AUTHORS:

Christian. Schoneich
University of Kansas
239 PUBLICATIONS **8,141** CITATIONS

SEE PROFILE

Todd D Williams
University of Kansas
133 PUBLICATIONS **4,093** CITATIONS

SEE PROFILE

Cu(II)-Catalyzed Oxidation of β-Amyloid Peptide Targets His^{13} and His^{14} over His^6: Detection of 2-Oxo-histidine by HPLC-MS/MS

Christian Schöneich*,† and Todd D. Williams‡

Department of Pharmaceutical Chemistry, The University of Kansas, 2095 Constant Avenue, Lawrence, Kansas 66047, and Mass Spectrometry Laboratory, The University of Kansas, Lawrence, Kansas 66045

Received January 2, 2002

The interaction of β-amyloid peptide (βAP) with Cu(II) leads to the formation of reactive oxygen species, neurotoxicity, and the chemical modification of the peptide. To study product formation and the potential selectivity of oxidation, we have exposed specific βAP congeners, βAP1−16, βAP1−28, and βAP1−40, to ascorbate/Cu(II)-induced metal-catalyzed oxidation and electrospray ionization-time-of-flight (ESI-TOF) MS/MS analysis. Incubation of 30 μM βAP with 15−150 μM Cu(II) and (physiologically relevant) 720 μM ascorbate in 20 mM phosphate buffer, pH 7.4, leads to significant oxidation of the peptides within remarkably short reaction times of as low as 6 min. Initial oxidation targets are His^{13} and His^{14}, which are converted to 2-oxo-His, whereas the other two metal-binding residues, His^6 and Tyr^{10}, remain intact. Longer oxidation times then also target His^6. Even in βAP1−40 the oxidation of His^{13} and His^{14} precedes the oxidation of Met^{35}. Especially, the insensitivity of Tyr^{10} is noteworthy and may be explained by electron withdrawal from the Tyr side chain through complexation of Cu(II). The insensitivity of His^6 to initial oxidation may be rationalized by a proposed bridging of two Cu(II)-βAP congeners, lowering the electron density on His^6, comparable to similar results on a Cu(II)- and Zn(II)-bridging His^{61} residue of bovine Cu,Zn superoxide dismutase.

Introduction

The deposition of β-amyloid peptide (βAP) into senile plaque is an important factor in the pathogenesis of Alzheimer's disease (*1*−*5*). While βAP1−40 represents the major circulating βAP sequence, the predominant sequence incorporated into plaque is βAP1−42 (*6*, *7*). An important hallmark of βAP is its pronounced tendency to aggregate, ultimately forming fibrils in which βAP adopts a β-sheet conformation (*8*−*13*). For some time, βAP aggregation has been considered the key parameter by which βAP formation influences the progression of Alzheimer's disease. However, increasing experimental evidence is mounting that aggregation may not be the only mechanism of βAP action (*14*−*23*). In 1994, Hensley et al. reported on the apparently spontaneous fragmentation of βAP, accompanied by the formation of free radicals (*14*). Subsequently, it was discovered that βAP binds Cu^{2+} and Zn^{2+} with very high affinity, and that the incubation of full-length βAP with Cu^{2+} leads to the reduction of Cu^{2+} to Cu^+ (*19*−*21*, *23*). This electron transfer depends on the simultaneous presence of three His residues in the N-terminus, His^6, His^{13}, and His^{14}, and Met^{35} in the C-terminus. However, thermodynamics and mechanism(s) of this electron transfer are presently unclear. Under aerobic conditions, the reduction of Cu^{2+} ultimately produces H_2O_2 (*20*), leading to the hypothesis that the βAP−Cu^{2+} interaction is a source for oxidative stress. In fact, Alzheimer's disease brain is characterized by elevated levels of oxidative stress and high levels of redox-active transition metals such as Cu and Fe (*24*−*26*). The simultaneous production of βAP-bound Cu^+ and H_2O_2 suggests that Fenton-type reactions may produce hydroxyl radicals (or their metal-bound equivalents) which may ultimately oxidize βAP or other biomolecules present in its vicinity. Supporting this hypothesis, the expression of native βAP1−42 in transgenic *C. elegans* leads to plaque formation, accompanied by significantly elevated levels of protein carbonyls, a marker for protein oxidation (*27*). Moreover, βAP isolated from human Alzheimer's disease brain shows a ca. 32% loss of its His residues, corresponding to ca. 1 mol of His/mol of βAP (*28*). Subsequent in vitro experiments have confirmed that βAP is indeed sensitive to metal-catalyzed oxidation (*28*).

It is known that transition metal-binding His residues are targets for site-specific metal-catalyzed protein oxidation (*29*−*37*), and the Alzheimer's disease-dependent loss of His indicates that βAP may suffer metal-catalyzed oxidation in vivo. However, neither oxidation products of His have been characterized nor the target His residues of βAP have been identified, and, therefore, such experiments are described in this paper. For the following mechanistic reasons, our experiments were performed predominantly with βAP1−28 ($D^1AEFR\mathit{H}^6DSG\mathit{Y}^{10}EV\mathit{H}^{13}\mathit{H}^{14}QKLVFFAEDVGSNK^{28}$). (i) βAP1−28 strongly binds Cu^{2+} as it contains all three His and one Tyr residue (Tyr^{10}) important for metal binding (*21*). (ii) βAP1−28 aggregates much slower than the longer chain βAP structures (*21*), i.e., βAP1−40 and βAP1−42, so that complications due to aggregation can be minimized,

* To whom correspondence should be addressed. Phone: (785) 864-4880. Fax: (785) 864-5736. E-mail: schoneic@ukans.edu.
† Department of Pharmaceutical Chemistry.
‡ Mass Spectrometry Laboratory.

10.1021/tx025504k CCC: $22.00
Published on Web 04/05/2002

especially during short reaction times. (iii) βAP1−28 lacks the methionine residue, Met^{35}, at the C-terminus, which represents an additional potential site of oxidation. Therefore, the ascorbate-dependent metal-catalyzed oxidation of βAP can be studied independent of a potential contribution of electron transfer from Met^{35}. (iv) βAP1−28 is a sufficiently short polypeptide, which, by analogy to our recent experiments with the B-chain of insulin (*35*), can be sequenced directly in the mass spectrometer by collision-induced fragmentation (CID) even without prior proteolytic digestion. Additional results are presented for βAP1−40, which is composed of βAP1−28 with a C-terminal tail, $G^{29}AIIGLMVGGVV^{40}$. In all experiments, ascorbate is the primary electron donor inducing the Cu^{2+}-catalyzed activation of oxygen. We will show for both βAP1−28 and βAP1−40 that the ascorbate-dependent metal-catalyzed oxidation of βAP primarily targets the metal-binding residues His^{13} and His^{14} in a site-specific process, but that the metal-catalyzed oxidation of Tyr^{10} and (for βAP1−40) Met^{35} is negligible.

Materials and Methods

Materials. βAP1−16, βAP1−28, and βAP1−40 were obtained from Bachem (King of Prussia, PA), and their purity and homogeneity checked by electrospray MS. Stock solutions of all peptides, [βAP1−16] = 5.1×10^{-4} M, [βAP1−28] = 3.06×10^{-4} M, and [βAP1−40] = 1.15×10^{-4} M, were prepared in deionized water (Millipore), and the stock solutions were immediately subjected to brief centrifugation in order to precipitate possible seeds for peptide aggregation. We observed little loss of peptide during the brief centrifugation and the time required to prepare the reaction mixtures. Sequencing grade modified trypsin was purchased from Promega (Madison, WI). All other chemicals were of the highest commercially available purity and used as received.

Reactions. Metal-catalyzed oxidation was initiated by exposure of βAP−Cu^{2+} complexes to ascorbate at room temperature. All reactions were performed in 100 μL volumes in 1 mL Teflon vials, which allows for sufficient oxygen in the headspace. The order of addition of the individual components of the reactions was as follows: an aliquot of βAP stock solution was diluted with water and phosphate buffer, and an aliquot of $CuCl_2$ added, before the reaction was started by the addition of ascorbate. Control experiments were performed in the absence of ascorbate. The reactions were stopped either by the addition of a final concentration of 1.0×10^{-3} M EGTA (to complex Cu^{2+}) or the addition of a final content of 1% (v/v) acetic acid. For the tryptic digestion of βAP, the reactions were first stopped by the addition of EGTA before the solutions were incubated for 40−80 min at room temperature with a 1:75 molar ratio of trypsin to βAP.

Sample Preparation for MS Analysis. Either undigested or trypsin-digested peptides (usually ca. 300 pmol) were trapped and desalted on a custom packed C18 1.0 × 20 mm column (Zorbax, 5 μm, 300 A). For loading of the column, a final concentration of 20% (v/v) acetic acid was added to the reaction mixtures, and the samples were slowly infused onto the column. Peptides were eluted into the mass spectrometer with an eluent consisting of 90% (v/v) MeOH, 10% water, and 0.5% formic acid.

Electrospray Ionization Time-of-Flight (ESI TOF) Analysis. ESI spectra were acquired on a Q-Tof-2 (Micromass Ltd., Manchester, U.K.) hybrid mass spectrometer operated in the MS1 mode and acquiring data with the time-of-flight analyzer. The instrument was operated for maximum resolution with all lenses optimized on the $[M + 2H]^{2+}$ ion from the cyclic peptide Gramicidin S. The cone voltage was 30 eV and Ar was admitted to the collision cell at a pressure that attenuates the beam to about 20% and the cell was operated at 5 eV (maximum transmission). Spectra were acquired at 11 364 Hz pusher frequency covering the mass range 100−2000 amu and accumulating data for 5 s per cycle. Time to mass calibration was made with CsI cluster ions acquired under the same conditions.

MS/MS Analysis. CID spectra were acquired by setting the MS1 quadrupole to transmit a precursor mass window of ±1.5 amu centered on the most abundant isotopomer. Ar was the collision gas admitted at a density that attenuates the beam to 20%; this corresponds to 16 psi on the supply regulator or 5.3×10^{-5} mBar on a penning gauge near the collision cell. The collision energy was 20 eV. Spectra were acquired for 2−3 min in 5 s cycles as the peptides were eluted off a desalting column. To obtain an unambiguous localization of the oxidation of specific amino acid residues, we carefully controlled all b and y″ fragments (for nomenclature, see below) for possible overlap with isobaric internal fragments.

Results

Oxidation Yields. The incubation of 30 μM βAP1−28 with 150 μM Cu^{2+} and 720 μM ascorbic acid in 20 mM phosphate buffer, pH 7.4, leads to a very rapid oxidation of the peptide within a few minutes. For example, Figure 1A reveals that, at 6 min after start of the oxidation, the reaction mixture contains ca. 29% monooxidized peptide, βAP1−28(+1O), 23% doubly oxidized peptide, βAP1−28-(+2O), 11% triply oxidized peptide, βAP1−28(+3O), with 37% native βAP1−28 remaining. Every addition of a single oxygen atom to the peptide is indicated by an increase of 16 atomic mass units (amu) relative to the mass of the native sequence. These relative yields change slightly upon oxidizing the peptide for an additional 10 min (Figure 1B). In control experiments, no oxidation is detected when βAP was incubated with Cu^{2+} in the absence of ascorbate.

Importantly, the presence of 1% (v/v) methanol in the reaction mixture does not inhibit the metal-catalyzed oxidation of βAP. One mechanism for the incorporation of oxygen into the peptide is the hydroxylation of aromatic amino acid residues such as His (*33*) and/or Tyr (*38*), potentially indicative of hydroxyl radicals and/or hydroxyl radical-like oxidants. Our experiment with methanol suggests that, if involved, hydroxyl radicals are reacting site specifically, in agreement with various studies on the Cu^{2+}-catalyzed oxidation of His in other proteins such as Cu,ZnSOD (*31*) and human growth hormone (*33*).

While 16 min of reaction produce high yields of oxidized βAP, our MS analysis reveals no significant formation (<3%) of covalently linked dimers, e.g., through formation of bityrosine.

A 6 min incubation of 30 μM βAP1−40 with 150 μM Cu^{2+} and 720 μM ascorbate in 20 mM phosphate buffer, pH 7.4, yields predominantly the monooxidized species βAP1−40(+1O), accounting for approximately 18% of the total peptide. Tryptic digestion of the peptide showed no significant oxidation of the tryptic fragments T_3 (Leu^{17}−Lys^{28}) and T_4 (Gly^{29}−Val^{40}), indicating that Met^{35} is not a primary target for the ascorbate-dependent metal-catalyzed oxidation. On the other hand, we detected significant yields of the tryptic fragment T_2, which was +16 amu heavier, i.e., T_2 + 16, together with native T_2 (His^6-Lys^{16}), indicating fairly selective incorporation of a single oxygen atom into T_2. A similar selectivity was observed during a 30 min incubation of 30 μM βAP1−40 with 15 μM Cu^{2+} (i.e., [βAP1−40]:[Cu^{2+}] = 2:1) and 720 μM ascorbate with no oxidation of T_3 and T_4 but formation of T_2 + 16 [under these conditions, ca. 6% of the

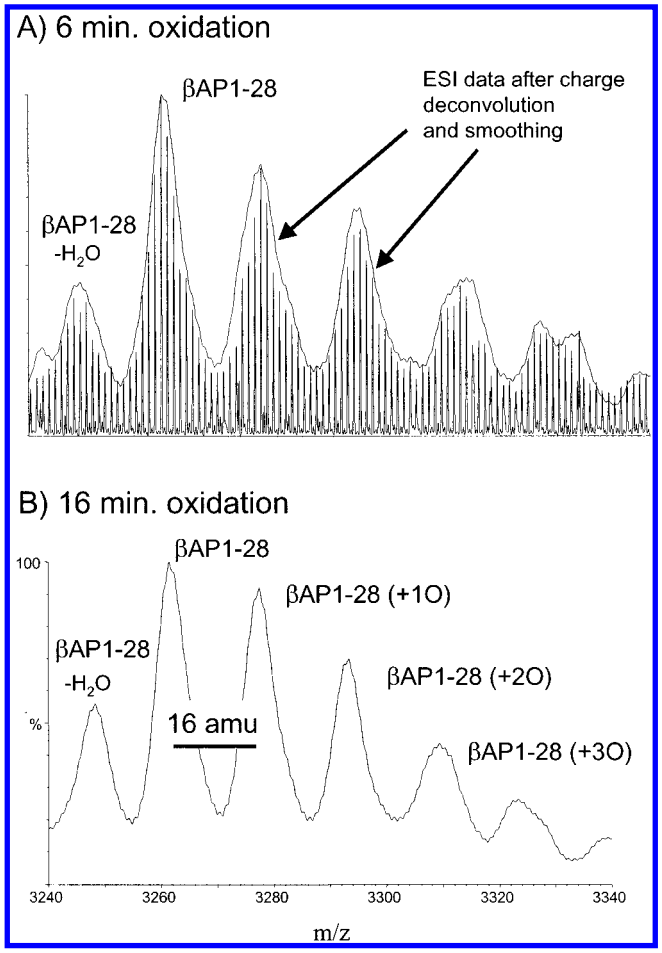

Figure 1. ESI mass spectra of βAP1−28 oxidized for (A) 6 min and (B) 16 min under the following conditions: air-saturated solutions of 30 μM βAP1−28, 150 μM Cu^{2+}, 720 μM ascorbate in 20 mM phosphate buffer, pH 7.4.

original peptide were converted to βAP1−40(+1O) within 30 min].

Oxidation of Met^{35} to Met sulfoxide is only observed after 30 min incubation of 30 μM βAP1−40 with 150 μM Cu^{2+} and 720 μM ascorbate, and prolonged tryptic digestion for 80 min. However, this process likely involves the reaction of H_2O_2 (formed during the reaction of ascorbate with Cu^{2+}) with the tryptic fragment T_4.

Localization of Oxidation Sites. To probe for selectivity of oxidation, we focused especially on the MS/MS analysis of monooxidized βAP. MS/MS spectra were acquired on the full-length βAP1−28(+1O) and βAP1−40(+1O) as well as βAP1−28(+1O) and βAP1−40(+1O), which had been subjected to tryptic digestion. For the comparison of full-length βAP1−28(+1O) with native βAP1−28, we used the $[M + 4H]^{4+}$ ion with *m/z* 816.2 for native βAP1−28 vs *m/z* 820.2 for βAP1−28(+1O). For the comparison of full-length βAP 1−40(+1O) with native βAP1−40 we used the $[M + 5H]^{5+}$ ion with *m/z* 866.8 for native βAP1−40 and *m/z* 869.9 for βAP1−40(+1O).

(1) *β*AP1−28. The CID spectra of the native peptide (*m/z* 816.2) are dominated by an intense b series, b_7−b_{23} (also the ions b_2−b_6 are observed albeit at lower intensities), and an abundant y series of y_3''−y_{11}'' (Figure 2). For a definition of the respective ion series b and y, see the nomenclature by Roepstorff and Fohlman (*39*). The term y″ denotes a y fragment with two added hydrogen atoms, i.e. y″ = y + 2H (*40*). Cleavage sites for b and y ions are illustrated in the insert of Figure 2. Comparison of the CID spectra of βAP1−28 and βAP1−28(+1O) after 16 min of oxidation localizes the addition of one oxygen atom (+16 amu) to the sequences Asp^1-His^6 and His^{13}-Lys^{17}. For example, the most abundant ions in the CID spectra of both peptides are those of the series y_3'' to y_{11}'' which are identical in mass and relative abundance for both peptides; therefore, the addition of +16 amu must occur between residues 1−17. The next most abundant ions are those of the b series. In βAP1−28(+1O) the ions b_6−b_{11} are reduced to ca. 55 ± 10% compared to b_6−b_{11} in native βAP1−28. Importantly, starting with b6 we detect additional fragments 16 amu higher in mass (e.g., b_6 + 16, b_7 + 16 etc.) which are absent in native βAP1−28. This is evidence for oxygen addition on His^6. Integration of the respective peak areas reveals ca. 30% oxidation of His^6. The next significant change occurs after Val^{12}. While the spectrum of βAP1−28(+1O) shows an abundant fragment b_{12}, corresponding to unmodified Val^{12}, the intensities of fragments b_{13} and b_{14} are significantly reduced again, to ca. 8 and 3% of their original intensities in the spectrum of native βAP1−28. However, they are replaced by fragments which are 16 amu higher in mass, i.e., b_{13} + 16 and b_{14} + 16. This result indicates oxygen addition at His^{13} and His^{14} (confirmed by more detailed investigations on tryptic peptides, presented below).

The hydroxylation of Tyr was excluded in the following way. Tyr hydroxylation would show through increased intensities of fragments b_{10} + 16, b_{11} + 16 and b_{12} + 16 compared to the intensities of b_6 + 16, b_7 + 16, and b_9 + 16 as well as the presence of an immonium ion of 3,4-dihydroxyphenylalanine. There was little convincing evidence for an increased intensity of fragments b_{10} + 16, b_{11} + 16, and b_{12} + 16 (also confirmed with tryptic peptides of oxidized βAP1−28, see below). Moreover, the quantitation of the 3,4-dihydroxyphenylalanine immonium ion (*m/z* 152) excluded Tyr hydroxylation at levels higher than 3% of the total oxidation yields. In conclusion, the analysis of 16 min-oxidized βAP1−28 shows oxidation of all His residues, His^6, His^{13}, and His^{14}, but excludes significant yields of Tyr hydroxylation. To obtain more information on the potential selectivity of oxidation during shorter reaction times, we extended our MS/MS analysis to βAP1−28 which had been oxidized for only 6 min.

Figure 3 shows a representative MS/MS analysis of the tryptic fragment T_2 of βAP1−28(+1O) after 6 min of oxidation. Fragment T_2 is obtained by cleavage C-terminal of Arg^5 and Lys^{16}, respectively. CID spectra, collected of the $[M + 3H]^{3+}$ ion of T_2 from native βAP1−28 (*m/z* 446.2), contain an extensive y series of y_2''−y_{10}'' and an abundant b series of b_2−b_{10} (the sequence of T_2 is shown in the inset in Figure 3; note that the fragment b_2 originates from cleavage of the peptide bond C-terminal of Asp^7 and the fragment y_2 through cleavage N-terminal of Gln^{15}). The most striking features of the CID spectra from T_2 of βAP1−28(+1O) (*m/z* 451.2) are the +16 amu shift in the y″ ions starting with y_3'' and the absence of any +16 amu shifts in the low mass b ions (up to b_7). For example, the signal with *m/z* 397.2 represents ion b_4, containing His^6, which is identical in mass and yield to b_4 from T_2 of native βAP1−28. There is no evidence for an ion with *m/z* 413.2, indicating that oxygen addition does not occur at His^6. Therefore, the b ions confine the addition of oxygen to amino acid residues His^{13}-Lys^{16} while the y + 16 ions further limit the oxygen

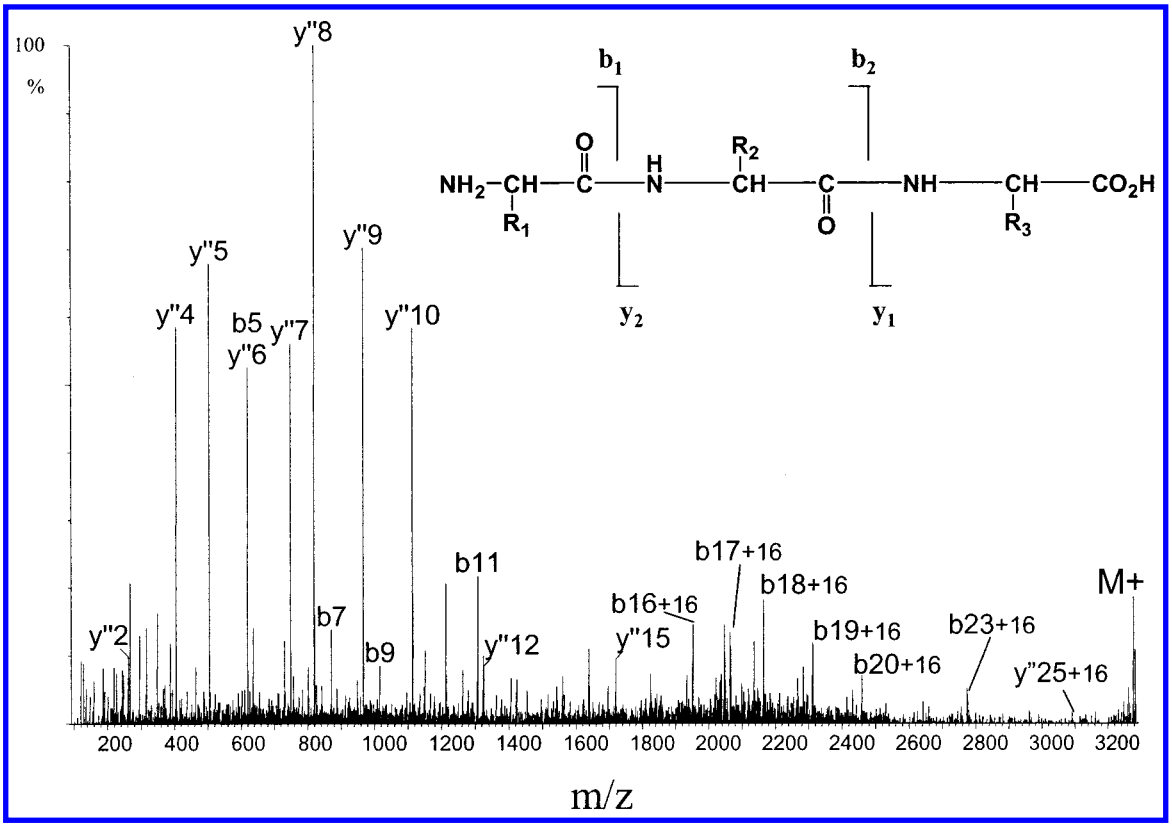

Figure 2. MS/MS spectrum of βAP1−28(+1O) with annotation of some of the observed fragments. A model peptide displaying the respective cleavage sites for b and y ions is shown in the insert. Usually, y ions add 2 hydrogen atoms to yield y + 2H = y″, and are detected as y″.

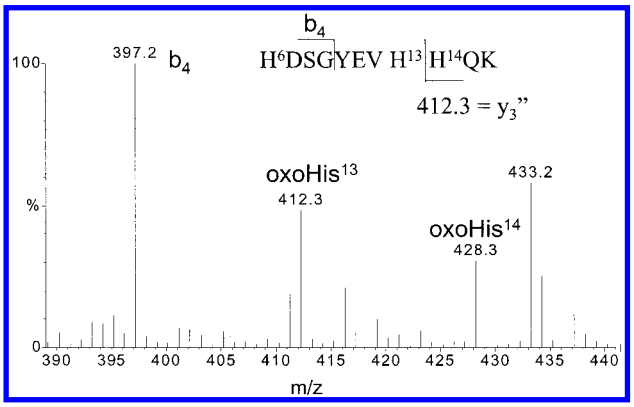

Figure 3. MS/MS spectrum of the tryptic fragment T_2 (H^6-K^{16}) of βAP1−28(+1O). Cleavage sites to generate the fragments b_4 and y_3'' are shown in the insert.

addition to His^{13} and His^{14}. These results exclude oxygen addition at His^6 and hydroxylation of Tyr^{10}. We obtain a ca. 1.6:1 ratio of the ions *m*/*z* 412.3 and 428.3, respectively. These represent the ions y_3'' and y_3'' + 16. By comparison to y_3'' from T_2 of native βAP1−28, we conclude that oxygen addition occurs to nearly equal extents at His^{13} and His^{14}. Hence, at earlier reaction times of 6 min, the Cu^{2+}-catalyzed oxidation of βAP1−28 targets nearly exclusively His^{13} and His^{14}. In control experiments, we verified that the tryptic digestion of βAP1−28(+1O) was complete and did not discriminate between peptide isoforms which were oxidized at His^{13} or His^{14} vs His^6. We observed a complete formation of T_1(1−5), T_2(6−16), and T_3(17−28) with little nondigested or incompletely digested βAP remaining. The net addition of one oxygen atom per His residue is consistent with the hydroxylation of His to 2-oxo-His by hydroxyl radicals (see Scheme 1).

Scheme 1

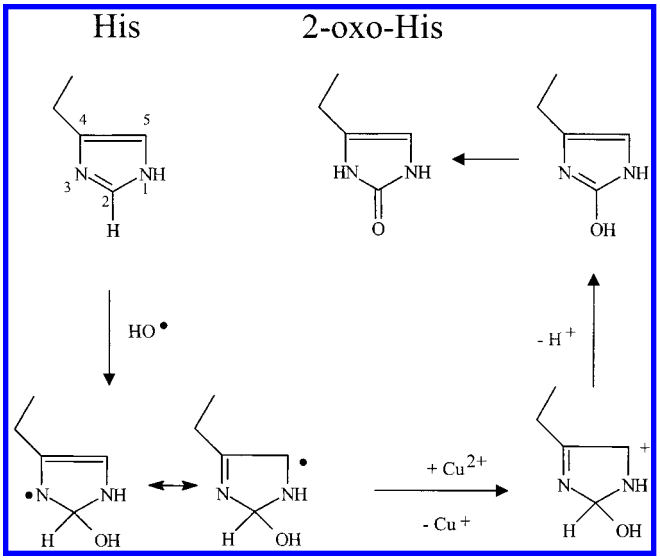

The formation of 2-oxo-His is corroborated by MS/MS detection of the immonium ion of 2-oxo-His (*m*/*z* 126).

Further evidence for the selective oxidation of His^{13} and His^{14} was obtained by exposing the shorter peptide βAP1−16 to metal-catalyzed oxidation for 6 min (30 μM peptide, 150 μM Cu^{2+}, and 720 μM ascorbate, pH 7.4). The results are identical to those obtained with the longer congener βAP1−28, i.e., exclusive oxidation of His^{13} and His^{14}.

(2) βAP1−40. The CID spectra of native βAP1−40 and βAP1−40(+1O) show an intense b and y series (as y″). Importantly, while the ion y_6'' is detectable, there is no evidence for the ion y_6'' + 16, indicating negligible oxygen

incorporation into the sequence $M^{35}VGGVV^{40}$. We detect all ions b_7-b_{12} with no convincing evidence for any ion +16 amu heavier, i.e., $(b_7-b_{12}) + 16$, indicating negligible oxygen incorporation into the sequence D^1-V^{12}, including His^6 and Tyr^{10}. However, starting with b_{13}, we see significant yields of ions, which are +16 amu heavier, i.e., $b_{13} + 16$, $b_{14} + 16$, etc. Hence, oxygen incorporation occurs at His^{13} and His^{14}, consistent with the results on βAP1−28 (see above). Hence, the ascorbate-dependent metal-catalyzed oxidation shows a similar selectivity for both βAP1−28 and βAP1−40.

Discussion

The Cu^{2+}-catalyzed oxidation of βAP1−16, βAP1−28, and βAP1−40 leads to the selective conversion of His to 2-oxo-His, indicated by oxygen addition to the invidual His residues and the formation of the 2-oxo-His immonium ion during CID experiments. On the basis of NMR and ESR experiments (*21*), it has been proposed that βAP binds Cu^{2+} via three His residues and Tyr^{10}. By analogy to findings with other proteins containing metal-binding His residues (*31*, *33*) we expected that the oxidation of βAP is ultimately carried out by Cu-bound hydroxyl radicals which convert His to 2-oxo-His in a site-specific process. This is confirmed by our result that 1% (v/v) methanol cannot protect βAP from the ascorbate-dependent metal-catalyzed oxidation. Recent data on the metal-catalyzed oxidation of bovine Cu,Zn superoxide dismutase (SOD) revealed significant oxidation of His^{44}, His^{46}, and His^{118}, all of which are coordinated only to one Cu^{2+}. However, only negligible oxidation was detected for His^{61}, which is coordinated to both Cu^{2+} and Zn^{2+}, possibly due to a decreased electron density on His^{61} caused by complexation to two Lewis acids (*32*). It has been suggested that complexation of βAP with Cu^{2+} and/or Zn^{2+} leads to allosterically ordered, α-helical structures (*21*). Moreover, the association of Cu^{2+}-complexed βAP peptides appears to be through a bridging His residue. By analogy to Cu,ZnSOD, the bridging His residue should be less sensitive to metal-catalyzed oxidation. The fact that the ascorbate-dependent Cu^{2+}-catalyzed oxidation of βAP predominantly targets His^{13} and/or His^{14}, but to a significantly lesser extent His^6, suggests that His^6 may be the bridging His residue, as originally proposed by Curtain et al. (*21*). The proposed coordination of Cu^{2+} to both N1 and N3 of the imidazole group of His^6 formally introduces positive partial charges on both nitrogens, resulting in a significant lowering of the electron density at C2, the position of hydroxyl radical attack leading to 2-oxo-His. Hence, coordination to two Cu^{2+} atoms can protect His^6 against attack by the electrophilic hydroxyl radical at C2, much as the bridging between Cu^{2+} and Zn^{2+} protects His^{61} in bovine Cu,ZnSOD (*32*). Oxidation of His^6 is only seen at longer reaction times. A possible explanation for this observation is that the initial oxidation of His^{13} and/or His^{14} may lead to changes in peptide conformation and/or Cu^{2+} complexation, eventually rendering His^6 more susceptible to oxidation with time.

The remarkable result that Tyr^{10} is not a target of metal-catalyzed oxidation (hydroxylation), though involved in Cu^{2+} complexation, may also be rationalized by electronic considerations. Complexation of Tyr^{10} via the phenolic/phenolate oxygen will certainly result in electron withdrawal from the aromatic ring, potentially lowering the rate constant for hydroxylation such that Cu^{2+}-complexed Tyr cannot compete for the hydroxyl radical against the surrounding His residues.

The rate of βAP oxidation is quite remarkable. Alzheimer's disease brain contains large amounts of Cu, especially in amyloid deposits where concentrations can reach up to 400 μM (*20*). Usually, brain levels of ascorbate are as high as 1.0 μmol/g tissue, corresponding to ascorbate concentrations on the order of 1 mM (*41*). Therefore, our reaction conditions with 15−150 μM Cu^{2+} and 720 μM ascorbate are physiologically relevant for Alzheimer's disease brains. Future experiments shall now yield information on whether βAP isolated from Alzheimer's disease brain shows selective or random His modification. Selective His modification (e.g., of His^{13} and His^{14}) would suggest that metal-catalyzed oxidation in vivo could stop short before targeting His^6, eventually leaving binuclear Cu complexes or higher aggregates intact.

Acknowledgment. This work was supported by the NIA (PO1AG12993).

References

(1) Selkoe, D. J. (1996) Amyloid β-protein and the genetics of Alzheimer's disease. *J. Biol. Chem.* **271**, 18295−18298.
(2) Wolfe, M. S., De Los Angeles, J., Miller, D. D., Xia, W., and Selkoe, D. J. (1999) Are presinilins intramembrane-cleaving proteases? Implications for the molecular mechanism of Alzheimer's disease. *Biochemistry* **38**, 11223−11230.
(3) Tanzi, R. E. (1999) A genetic dichotomy model for the inheritance of Alzheimer's disease and common age-related disorders. *J. Clin. Invest.* **104**, 1175−1179.
(4) Xia, W., Ray, W. J., Ostaszewski, B. L., Rahmati, T., Kimberley, W. T., Wolfe, M. S., Zhang, J., Goate, A. M., and Selkoe, D. J. (2000) Presinilin complexes with the C-terminal fragments of amyloid precursor protein at the sites of amyloid β-protein generation. *Proc. Natl. Acad. Sci. U.S.A.* **97**, 9299−9304.
(5) Martin, G. M. (2000) Molecular mechanisms of late life dementias. *Exp. Gerontol.* **35**, 439−443.
(6) Haass, C., Koo, E. H., Mellon, A., Hung, A. Y., and Selkoe, D. J. (1992) Targeting of cell-surface β-amyloid precursor protein to lysosomes: alternative processing into amyloid-bearing fragments. *Nature* **357**, 500−503.
(7) Seubert, P., Vigo-Pelfrey, C., Esch, F., Lee, M., Dovey, H., Davis, D., Sinha, S., Schlossmacher, M., Whaley, J., and Swindlehurst, C. (1992) Isolation and quantification of soluble Alzheimer's β-peptide from biological fluids. *Nature* **359**, 325−327.
(8) Bush, A. I., Pettingell, W. H., Multhaup, G. d., Paradis, M., Vonsattel, J.-P., Gusella, J. F., Beyreuther, K., Masters, C. L., and Tanzi, R. E. (1994) Rapid induction of Alzheimer Aβ amyloid formation by zinc. *Science* **265**, 1464−1467.
(9) Shen, C.-L., and Murphy, R. M. (1995) Solvent effects on self-assembly of β-amyloid peptide. *Biophys. J.* **69**, 640−651.
(10) Walsh, D. M., Lomakin, A., Benedek, G. B., Condron, M. M., and Teplow, D. B. (1997) Amyloid β-protein fibrillogenesis. *J. Biol. Chem.* **272**, 22364−22372.
(11) Tjernberg, L. O., Callaway, D. J. E., Tjernberg, A., Hahne, S., Lilliehöök, C., Terenius, L., Thyberg, J., and Nordstedt, C. (1999) A molecular model of Alzheimer amyloid β-peptide fibril formation. *J. Biol. Chem.* **274**, 12619−12625.
(12) Sipe, J. D., and Cohen, A. S. (2000) History of the amyloid fibril. *J. Struct. Biol.* **130**, 88−98.
(13) Kisilevski, R. (2000) Amyloidogenesis-unquestioned answers and unanswered questions. *J. Struct. Biol.* **130**, 99−108.
(14) Hensley, K., Carney, J. M., Mattson, M. P., Aksenova, M., Harris, M., Wu, J. F., Floyd, R. F., and Butterfiled, D. A. (1994) A model for β-amyloid aggregation and neurotoxicity based on free radical generation by the peptide: relevance to Alzheimer disease. *Proc. Natl. Acad. Sci. U.S.A.* **91**, 3270−3274.
(15) Harris, M. E., Hensley, K., Butterfield, D. A., Leedle, R. A., and Carney, J. M. (1995) Direct evidence for oxidative injury produced by the Alzheimer's β-amyloid peptide (1−40) in cultured hippocampal neurons. *Exp. Neurol.* **131**, 193−202.
(16) Butterfield, D. A. (1997) β-Amyloid-associated free radical oxidative stress and neurotoxicity: implications for Alzheimer's disease. *Chem. Res. Toxicol.* **10**, 495−506.

(17) Mattson, M. P., Mark, R. J., Furukawa, K., and Bruce, A. J. (1997) Disruption of brain cell ion homeostasis in Alzheimer's disease by oxy radicals, and signaling pathways that protect therefrom. *Chem. Res. Toxicol.* **10**, 507−517.

(18) Sayre, L. M., Zagorski, M. G., Surewicz, W. K., Krafft, G. A., and Perry, G. (1997) Mechanisms of neurotoxicity associated with amyloid β deposition and the role of free radicals in the pathogenesis of Alzheimer's disease: a critical appraisal. *Chem. Res. Toxicol.* **10**, 518−526.

(19) Huang, X., Cuajungco, M. P., Atwood, C. S., Hartshorn, M. A., Tyndall, J. D., Hanson, G. R., Stokes, K. C., Leopold, M., Multhaup, G., Goldstein, L. E., Scarpa, R. C., Saunders, A. J., Lim, J., Moir, R. D., Glabe, C., Bowden, E. F., Masters, C. L., Fairlie, D. P., Tanzi, R. E., and Bush, A. I. (1999) Cu(II) potentiation of alzheimer Aβ neurotoxicity. Correlation with cell-free hydrogen peroxide production and metal reduction. *J. Biol. Chem.* **274**, 37111−37116.

(20) Huang, X., Atwood, C. S., Hartshorn, M. A., Multhaup, G., Goldstein, L. E., Scarpa, R. C., Cuajungco, M. P., Gray, D. N., Lim, J., Moir, R. D., Tanzi, R. E., and Bush, A. I. (1999) The Aβ peptide of Alzheimer's disease directly produces hydrogen peroxide through metal ion reduction. *Biochemistry* **38**, 7609−7616.

(21) Curtain, C. C., Ali, F., Volitakis, I., Cherny, R. A., Norton, R. S., Beyreuther, K., Barrow, C. J., Masters, C. L., Bush, A. I., and Barnham, K. J. (2001) Alzheimer's disease amyloid-β binds copper and zinc to generate an allosterically ordered membrane-penetrating structure containing superoxide-dismutase-like subunits. *J. Biol. Chem.* **276**, 20466−20473.

(22) Varadarajan, S., Yatin, S., Aksenova, M., and Butterfield, D. A. (2000) Alzheimer's amyloid β-peptide-associated free radical oxidative stress and neurotoxicity. *J. Struct. Biol.* **130**, 184−208.

(23) Varadarajan, S., Kanski, J., Aksenova, M., Lauderback, C., and Butterfield, D. A. (2001) Different mechanisms of oxidative stress and neurotoxicity for Alzheimer's Aβ(1−42) and Aβ(25−35). *J. Am. Chem. Soc.* **123**, 5625−5631.

(24) Smith, M. A., Harris, P. L. R., Sayre, L. M., and Perry, G. (1997) Iron accumulation in Alzheimer disease is a source of redox-generated free radicals. *Proc. Natl. Acad. Sci. U.S.A.* **94**, 9866−9868.

(25) Smith, M. A., Hirai, K., Hsiao, K., Papolla, M. A., Harris, P. L. R., Siedlak, S. L., Tabaton, M., and Perry, G. (1998) Amyloid-β deposition in Alzheimer transgenic mice is associated with oxidative stress. *J. Neurochem.* **70**, 2212−2215.

(26) Sayre, L. M., Perry, G., Harris, P. L. R., Liu, Y., Schubert, K. A., and Smith, M. A. (2000) In situ oxidative catalysis by neurofibrillary tangles and senile plaques in Alzheimer's disease: a central role for bound transition metals. *J. Neurochem.* **74**, 270−279.

(27) Yatin, S. M., Varadarajan, S., Link, C. D., and Butterfield, D. A. (1999) In vitro and in vivo oxidative stress associated with Alzheimer's amyloid β-peptide (1−42). *Neurobiol. Aging* **20**, 325−330.

(28) Atwood, C. S., Huang, X., Khatri, A., Scarpa, R. C., Kim, Y.-S., Moir, R. D., Tanzi, R. E., Rohrer, A. E., and Bush, A. I. (2000) *Cell. Mol. Biol.* **46**, 777−783.

(29) Farber, J. M., and Levine, R. L. (1986) Sequence of a peptide susceptible to mixed-function oxidation. Probable cation binding site in glutamine synthetase. *J. Biol. Chem.* **261**, 4574−4578.

(30) Lewisch, S. A., and Levine, R. L. (1995) Determination of 2-oxohistidine by amino acid analysis. *Anal. Biochem.* **231**, 440−446.

(31) Uchida, K., and Kawakishi, S. (1994) Identification of oxidized histidine generated at the active site of Cu,Zn-superoxide dismutase exposed to H_2O_2. *J. Biol. Chem.* **269**, 2405−2410.

(32) Kurahashi, T., Miyazaki, A., Suwan, S., and Isobe, M. (2001) Extensive investigations on oxidized amino acid residues in H_2O_2-treated Cu,Zn-SOD protein with LC-ESI-Q-TOF-MS, MS/MS for the determination of the copper-binding site. *J. Am. Chem. Soc.* **123**, 9268−9278.

(33) Zhao, F., Ghezzo-Schöneich, E., Aced, G. I., Hong, J., Milby, T., and Schöneich, Ch. (1997) Metal-catalyzed oxidation of histidine in human growth hormone. *J. Biol. Chem.* **272**, 9019−9029.

(34) Hovorka, S. W., Williams, T. D., and Schöneich, Ch. (2002) Characterization of the metal-binding site of bovine growth hormone through site-specific metal-catalyzed oxidation and high-performance liquid chromatography-tandem mass spectrometry. *Anal. Biochem.* **300**, 206−211.

(35) Hovorka, S. W., Biesiada, H., Williams, T. D., Hühmer, A. F. R., and Schöneich, Ch. (2002) High sensitivity of Zn^{2+}-insulin to metal-catalyzed oxidation: detection of 2-oxo-histidine by MS/MS. *Pharm. Res.* **19**, 530−537.

(36) Mylonas, M., Malandrinos, G., Plakatouras, J., Hadjiliadis, N., Kasprzak, K. S., Krężel, A., and Bal, W. (2001) Stray Cu(II) may cause oxidative damage when coordinated to the -TESHHK-sequence derived from the C-terminal tail of histone H2A. *Chem. Res. Toxicol.* **14**, 1177−1183.

(37) Requena, J., Groth, D., Legname, G., Stadtman, E. R., Prusiner, S. B., and Levine, R. L. (2001) Copper-catalyzed oxidation of the recombinant SHa(29−231) prion protein. *Proc. Natl. Acad. Sci. U.S.A.* **98**, 7170−7175.

(38) Gieseg, S. P., Simpson, J. A., Charlton, T. S., Duncan, M. W., and Dean, R. T. (1993) Protein-bound 3,4-dihydroxyphenylalanine is a major reductant formed during hydroxyl radical damage to proteins. *Biochemistry* **32**, 4780−4786.

(39) Roepstorff, P., and Fohlman, J. (1984) Proposal for a common nomenclature for sequence of ions in mass spectra of peptides. *Biomed. Mass Spectrom.* **11**, 601.

(40) Snyder, P. A. (2000) *Interpreting protein mass spectra*, American Chemical Society, Washington, DC.

(41) Mårtensson, J., Han, J., Griffith, O. W., and Meister, A. (1993) Glutathione ester delays the onset of scurvy in ascorbate-deficient guinea pigs. *Proc. Natl. Acad. Sci. U.S.A.* **90**, 317−321.

TX025504K